Journal of Biological Physics (2023) 49:309–327
https://doi.org/10.1007/s10867-023-09632-4

RESEARCH

Evaluation of copper-induced biomolecular changes in different porin mutants of *Escherichia coli* W3110 by infrared spectroscopy

Gulcin Cetin Kilicaslan[1] · **Rafig Gurbanov**[2,3] · **Cihan Darcan**[1]

Received: 25 December 2022 / Accepted: 12 March 2023 / Published online: 3 April 2023

Abstract
Copper (Cu), one of the heavy metals, plays a vital role in many complex biochemical reactions as a trace element. However, it often becomes toxic when its concentration in the cell exceeds a certain level. Homeostasis of metals in the cell is primarily related to regulating metal transport into and out of the cell. Therefore, it is thought that porin proteins, which have a role in membrane permeability, may also play a role in developing Cu resistance. This study identified the differences between the molecular profiles of wild-type *Escherichia coli* W3110 and its seven different porin mutants exposed to Cu ions using attenuated total reflectance (ATR)–Fourier transform infrared (FTIR) spectroscopy. The results showed that the absence of porin genes elicits global changes in the structure and composition of membrane lipids and proteins, in both the absence and presence of Cu. The lack of porin genes significantly elevated the amounts of fatty acids and phospholipids. When the alterations in protein secondary structures were compared, the quantity of amide I proteins was diminished by the presence of Cu. However, the amount of amide II proteins increased in porin mutant groups independent of Cu presence or absence. The DNAs are transformed from B- and Z-form to A-form due to porin mutations and the presence of Cu ions. The lack of porin genes increased polysaccharide content independent of Cu presence. This study can help characterize Cu detoxification efficiency and guide for obtaining active living cells to be used in bioremediation.

Keywords *E. coli* W3110 · Porins · Infrared spectroscopy · Copper (Cu)

1 Introduction

Metals are essential for living organisms as they act as structural or catalytic components of biomolecules [1, 2]. Despite their critical role in cellular reactions, metals show toxic properties when their concentration exceeds a certain level [3]. Therefore, regulating the metal

✉ Rafig Gurbanov
rafiq.qurbanov@gmail.com

[1] Bilecik Şeyh Edebali University, Faculty of Science, Department of Molecular Biology and Genetics TR, Bilecik, TR 11100, Türkiye

[2] Bilecik Şeyh Edebali University, Faculty of Engineering, Department of Bioengineering, Bilecik, TR 11100, Türkiye

[3] Bilecik Şeyh Edebali University, Central Research Laboratory, Bilecik, TR 11100, Türkiye

concentrations is extremely important for cellular activities [4, 5]. Waste materials produced by industrial production contain large amounts of heavy metals. The direct discharge of this type of waste material into the environment increases the metal concentration in the ecosystem. With this increase, heavy metals accumulating in nature have become one of the most critical environmental problems negatively affecting the life of organisms [6, 7].

Bacteria have complex metal homeostasis mechanisms to maintain the sensitive balance between metal starvation and toxicity [8]. When the extracellular concentration of a particular metal increases, bacteria must first inhibit metal entry to maintain metal homeostasis and prevent cellular damage [3]. In Gram-negative bacteria, the outer membrane is the first barrier to metal penetration into the cell. It is provided by the outer membrane proteins that enable or prevent the penetration of the metal into the cell [9]. Porin proteins in the outer membrane are water-filled channels that allow the uptake of hydrophilic compounds smaller than 600 kDa through their central holes and show specific or non-specific permeability [10]. Therefore, it is thought that porin proteins may have a role in developing metal resistance.

Bacteria adapt to the environment by altering various metabolic pathways to survive under heavy metal concentrations [11, 12]. During this adaptation, the structure and functionality of all cellular molecules have been reported to be modified [13, 14]. Attenuated total reflectance (ATR)–Fourier transform infrared (FTIR) spectroscopy, a fast, inexpensive, and easy method, is often used to study these biomolecular modifications [15]. Spectral data obtained from ATR-FTIR spectroscopy provide essential information about the biochemical composition of the bacterial cell [16, 17]. ATR-FTIR spectroscopy is generally used for separating, classifying, and identifying bacteria [18–21]. However, it has recently started to be used in many different areas of bacterial research. For example, bacteria's functional and chemical composition can be identified without damaging biological samples such as bacterial cellulose or bio-cellulose [22, 23]. Moreover, studies show that ATR-FTIR spectroscopy can rapidly identify heavy metal-resistant bacteria and is used to identify molecular changes in lipids, proteins, and nucleic acids of bacteria exposed to lead and cadmium metals [24]. Furthermore, the cell wall structures of bacteria are specialized to provide metal detoxification by the presence of various surface organic functional groups with high affinity for metal binding. FTIR spectroscopy has also been used to identify these functional groups [25, 26].

The increasing heavy metal pollution in the environment has become a threat to the health of living things, and there is a growing trend to obtain bacterial strains that can be used for bioremediation processes [27]. Gram-negative bacteria have an extra membrane, called the outer membrane, that protects itself against various environmental conditions [28]. Many porin proteins' functions have been determined, comprising about half of the outer membrane. The leading porins of these proteins, OmpF and OmpC, are associated with permeability and lead to the transport of ions, nutrient molecules, amino acids, and sugars across the outer membrane [29]. In addition, different roles of ompA, which functions in the integrity of the bacterial cell surface [30, 31], such as participating in biofilm formation and acting as a receptor for several bacteriophages, have been determined [32]. The literature shows that the mechanism of porin synthesis is very complex, and factors such as starvation, pH, and temperature are involved in the transcriptional and translational control of porins [33–35].

Porins are water-filled channels formed in the ß-barrel structure that allow hydrophilic molecules in the outer membrane to be transported across the membrane [36, 37]. Any change in these structures directly alters the pore structure and causes the molecules entering the cell to change [38]. There are many studies on this subject. Low et al. [39] studied *Escherichia coli* strains exposed to different antibiotics and determined two mutations in

the OmpC porin of resistant cells. Similarly, studies conducted in *E. aerogenes* [40] and *Neisseria gonorrhoeae* species [41] determined that the decrease in antibiotic susceptibility resulted from changes in porin proteins. The study by Bouffartigues et al. [42] reported that the deletion of the porin gene supports biofilm formation. In contrast, the study by Ruffing determined that the production of fatty acids increased in the porin mutant bacteria [40]. They showed that specific lipopolysaccharide (LPS) domains are essential in placing porins on the outer membrane and that these interactions form mechanisms that maintain the stability and impermeability of the outer membrane [41]. Moreover, in studies, the metal resistance processes in bacteria were chiefly determined by investigating the expression profiles of candidate genes in the presence of metal stress [42–44]. However, how the absence of porin genes affects biomolecules in the cell under metal stress is not yet known. Therefore, this study aimed to elucidate the biomolecular changes in wild-type *Escherichia coli (E. coli)* W3110 and its seven different porin mutants (*ompA*, *ompC*, *ompF*, *ompG*, *ompT*, *lamB*, and *phoE*) both in the presence and absence of copper (Cu) ions by using ATR-FTIR spectroscopy.

2 Materials and methods

2.1 E. coli strains used in the study

The wild-type *E. coli* W3110 and *E. coli* BW25113 mutant strains were obtained from the Keio collection of the National Institute of Genetics of Japan. The target seven-gene region from *E. coli* BW25113 strains was transferred to wild-type *E. coli* W3310 using the P1kc phage transduction method and used in studies [45, 46]. Wild-type *E. coli* W3110 and mutant cells used in this study, shown in Table 1 and found in the microorganism collection, are currently stored in a deep freezer at −80 °C.

2.2 Bacterial growth conditions

The stock solution of $CuSO_4$ metal used in growth was prepared by dissolving in water to 0.2 M and was sterilized by the 0.22-µm pore-size filter membrane. Minimal inhibition concentration (MIC) and minimal bactericidal concentration (MBC) values of Cu against wild-type and mutant cells were determined [47]. In metal-containing growth experiments,

Table 1 *E. coli* W3110 strains used in the study

Laboratory stock number	Genotype	Source
W3110	Wild type	
CD200	W3110 *ompA::km*	It was achieved in the research project numbered 2015–01.BŞEÜ.04–02
CD201	W3110 *ompC::km*	It was achieved in the research project numbered 2015–01.BŞEÜ.04–02
CD202	W3110 *ompF::km*	It was achieved in the research project numbered 2015–01.BŞEÜ.04–02
CD203	W3110 *ompG::km*	It was achieved in the research project numbered 2015–01.BŞEÜ.04–02
CD204	W3110 *ompT::km*	It was achieved in the research project numbered 2015–01.BŞEÜ.04–02
CD205	W3110 *lamB::km*	It was achieved in the research project numbered 2015–01.BŞEÜ.04–02
CD206	W3110 *phoE::km*	It was achieved in the research project numbered 2015–01.BŞEÜ.04–02

the metal stock solution was added to the media at a concentration ¾ times the MIC value of wild-type *E. coli* W3110. Wild-type *E. coli* W3110 and mutant strains were incubated for 18 h at 37 °C in test tubes containing 5 ml of Luria–Bertani (L.B.) broth. The density of bacteria was adjusted to 0.005 absorbance value at OD_{600} in flasks containing 15 ml of L.B. Growth experiments were carried out with the addition of metal in one set and the absence of metal in the other. In metal-containing growth experiments, a Cu stock solution was added to the media at a final concentration of 2.8 Mm. Wild-type *E. coli* W3110 and W3110 mutant strains were grown at 37 °C under aerobic conditions in an orbital shaker at 160 rpm for 8 h. As a result of incubation, each sample of 1 ml was taken from the grown cells. The bacterial suspensions were centrifuged for 10 min at 10,000 *g*. The supernatants were removed, and pellets were washed twice with 1 ml of 1X PBS buffer. PBS was removed entirely from the samples.

2.3 IR spectroscopy experiments and data analyses

The IR spectra of bacteria were obtained using Frontier FTIR Spectrometer (PerkinElmer, USA) equipped with a universal ATR Miracle accessory. The grown cell pellets were resuspended in 100 µl of distilled water. The spectrum of air was used as a reference. A total of 10 µL of the sample was placed on a diamond/ZnSe crystal plate (PerkinElmer, USA). The bacteria were scanned over the spectral range 4000 to 650 cm^{-1} with a resolution of 4 cm^{-1} and 32 scans at room temperature. The second derivative IR spectra were used in all spectral analyses.

3 Results and discussion

This study showed biomolecular changes in wild-type *E. coli* (W3110) and its seven different porin mutants (*ompA*, *ompC*, *ompF*, *ompG*, *ompT*, *lamB*, and *phoE*) were comparatively investigated in both the presence and absence of Cu ions. Our previous study determined Cu's minimum inhibitory concentration (MIC) as 936 µg/ml for wild-type *E. coli* W3110 (Table 3). The metal stock solution was added to the media at a concentration ¾ times MIC value according to wild-type *E. coli* W3110 of metals in metal-containing growth experiments, and a growth curve was drawn (Fig. 1). Therefore, bacteria were grown in media containing 75% (2.8 mM) Cu of the minimum inhibitory concentration. Subsequently, the structural and functional changes in biomolecules of *E. coli* and its porin mutants were compared with infrared (I.R.) spectroscopy depending on Cu exposure. The spectra of unexposed (control group), Cu-exposed *E. coli*, and corresponding porin mutants were examined in the entire IR region (4000–650 cm^{-1}). The detected spectral bands were analyzed in 4 main areas consisting of lipids (3100–2800 cm^{-1}), fingerprint (diverse region: fatty acids, proteins, and lipid/1800–1400 cm^{-1}), nucleic acids (1250–1200 cm^{-1}), and polysaccharides (1100–1000 cm^{-1}) (Figs. 2–7). The assignments of these detected bands are given in Table 2.

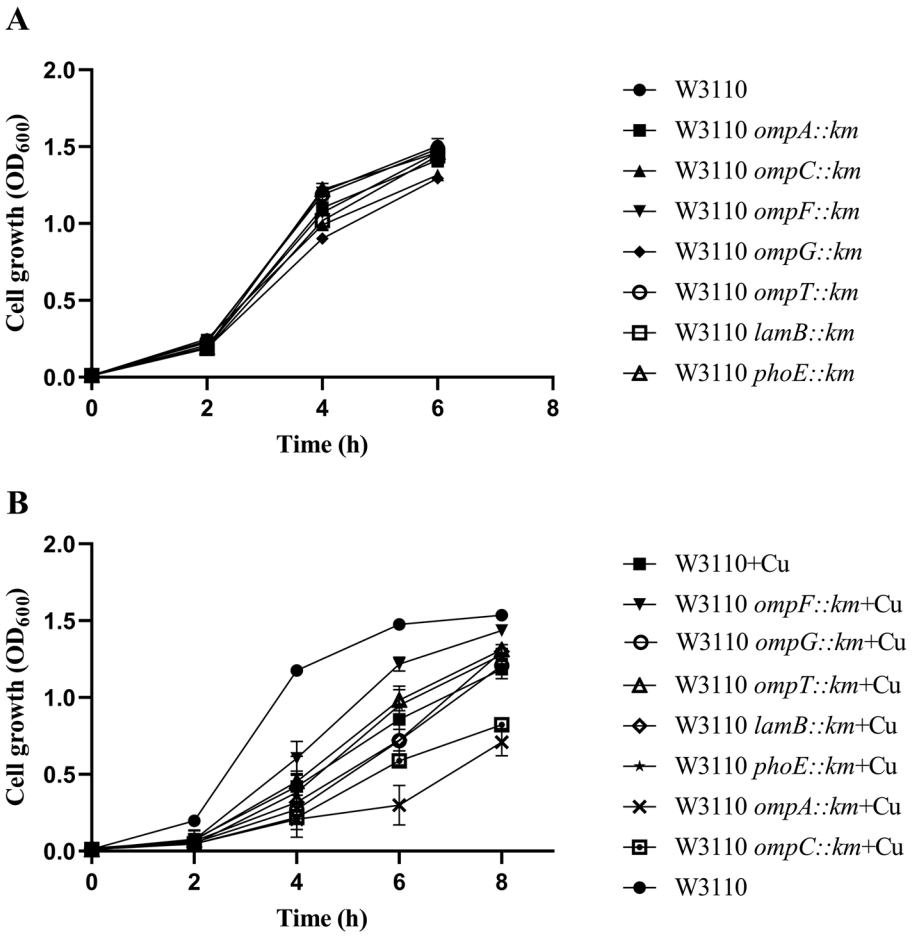

Fig. 1 Growth curve of the wild-type *E. coli* (W3110) and *E. coli* porin mutants in the absence (**A**) and presence (**B**) of Cu ions

3.1 Porin mutations alter the bacterial lipids in the presence and absence of copper ions

The spectral bands located at the 3100–2800 cm^{-1} region were analyzed to determine the variations in the lipid constituents of Cu-exposed and unexposed bacteria (Fig. 2). In a metal-free medium, the area of the band at 3011 cm^{-1} associated with the unsaturated lipids diminished in porin mutant cells compared to the wild type (Fig. 2A). However, with the addition of Cu, this band shifts to 3013 cm^{-1} position in wild-type *E. coli* W3110. Moreover, its area increases in all porin-mutant bacterial groups (Fig. 2B). The analysis of the band at 2918 cm^{-1} associated with CH_2 antisymmetric stretching of lipid molecules revealed an increase in the lipid quantity in all porin-mutant bacteria compared to the wild type regardless of the metal absence or presence (Fig. 2C, D). Therefore, this increase in lipid content is suggested to be associated with the lack of porin genes, not due to Cu ions (Table 3). The number of lipids forming the spectral band at 2850 cm^{-1} (CH_2 symmetric stretching) increased in porin mutants of *E. coli* compared to the wild-type strain, in the

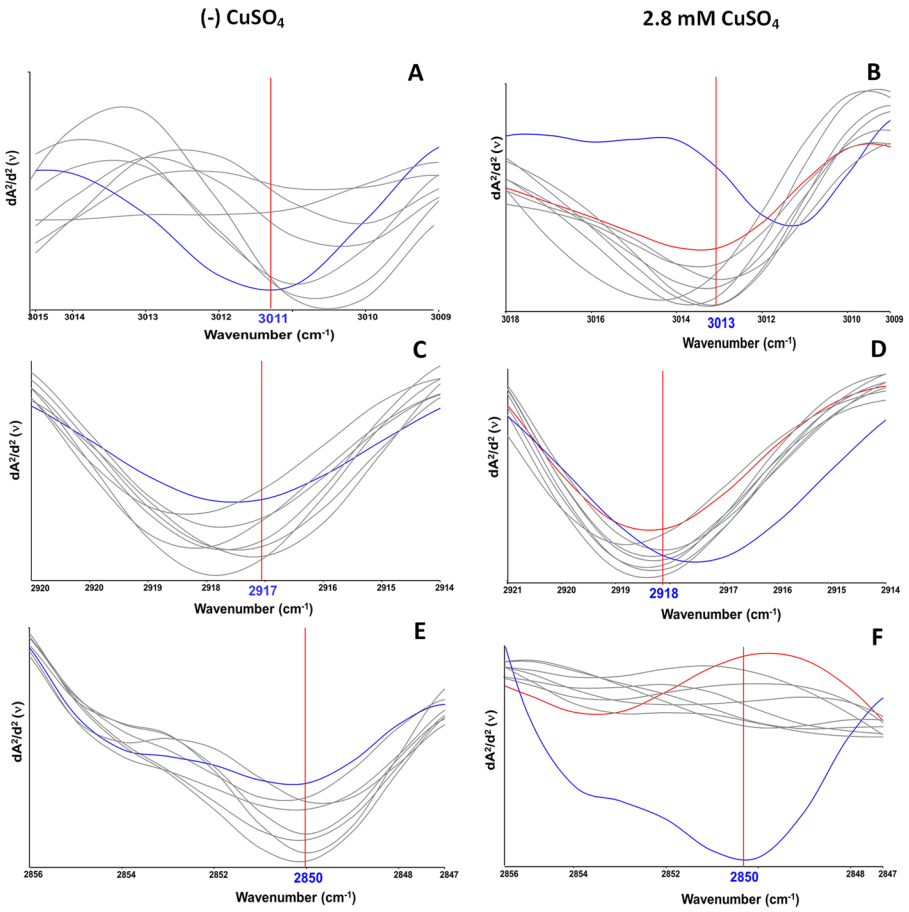

Fig. 2 Average second derivative and baseline-corrected infrared spectra of the wild-type *E. coli* (W3110) and *E. coli* porin mutants in the absence and/or presence of Cu ions for 3011–13 cm^{-1} (**A**, **B**), 2917 cm^{-1} (**C**, **D**), and 2850 $cm.^{-1}$ (**E**, **F**) spectral bands. Blue line: wild-type *E. coli* (W3110) in the absence of Cu ions. Red line; wild-type *E. coli* (W3110) in the presence of Cu ions. Gray line: *E. coli* porin mutants in the absence (**A**, **C**, and **E**) and presence of Cu ions (**B**, **D**, and **F**)

absence of Cu (Fig. 2F). However, this band disappeared in the presence of Cu (Fig. 2F) showing that the concentrations of lipids decrease. Studies using FTIR on various bacteria determined a significant decrease in lipids due to treatment with Cu, Zn, and Ag [24, 48, 49].

3.2 Porin mutations alter bacterial fatty acids in the presence and absence of copper ions

The spectral bands located at 1800–1700 cm^{-1} spectral region were evaluated to determine the changes in fatty acids of Cu-exposed and unexposed bacteria (Fig. 3). The triacylglycerols (T.G.s) constituting the 1743 cm^{-1} spectral band (C = O stretching mode of lipids) generally increased in the porin mutants when compared with the wild-type strain in the absence of Cu ions (Fig. 3A). However, the T.G. amount was severely

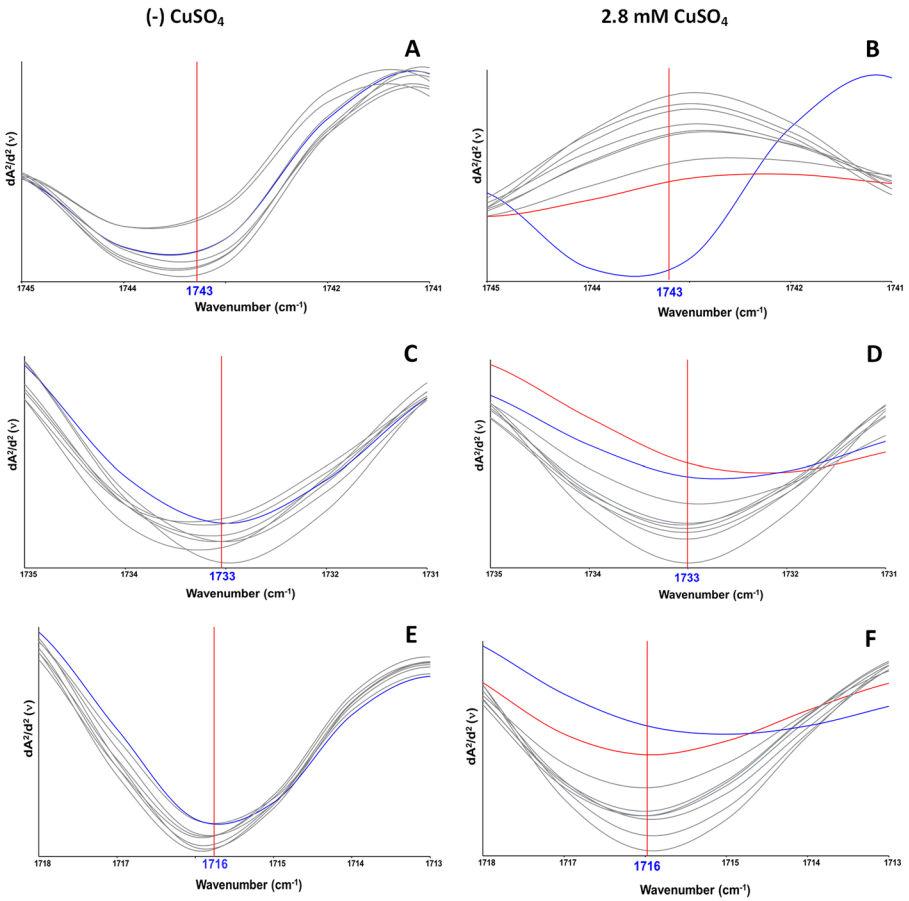

Fig. 3 Average second derivative and baseline-corrected infrared spectra of the wild-type *E. coli* (W3110) and *E. coli* porin mutants in the absence and/or presence of Cu ions for 1743 cm^{-1} (**A**, **B**), 1733 cm^{-1} (**C**, **D**), and 1716 $cm.^{-1}$ (**E**, **F**) spectral bands. Blue line: wild-type *E. coli* (W3110) in the absence of Cu ions. Red line; wild-type *E. coli* (W3110) in the presence of Cu ions. Gray line: *E. coli* porin mutants in the absence (**A**, **C**, and **E**) and presence of Cu ions (**B**, **D**, and **F**)

diminished in both wild-type and porin mutants in the presence of Cu ions (Fig. 3B). This decrease is probably due to Cu ions, not because of porin mutations. The bands at 1733 and 1716 cm^{-1} positions are associated with C = O stretching of lipid esters and phospholipids, respectively. Both bands' variation is similar and directly related to the porin mutations (Fig. 3C–F). In other words, the absence of porin genes increases the number of phospholipids independent of Cu ions.

3.3 Porin mutations alter bacterial proteins in the presence and absence of copper ions

To determine the changes in the proteins of Cu-exposed and unexposed bacteria, the amide I region located at 1700–1600 cm^{-1} spectral region consisting of proteins was evaluated (Fig. 4). While the band at 1652 cm^{-1} is due to stretching vibrations of C-O, which is a

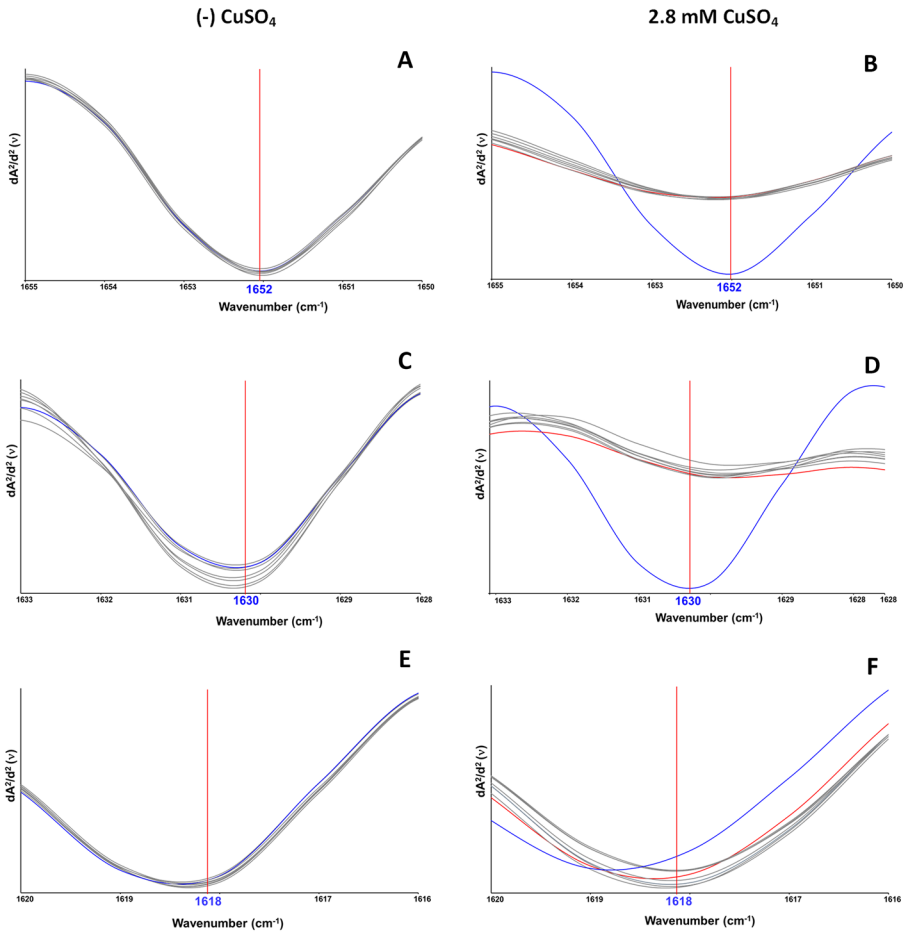

Fig. 4 Average second derivative and baseline-corrected infrared spectra of the wild-type *E. coli* (W3110) and *E. coli* porin mutants in the absence and/or presence of Cu ions for 1652 cm^{-1} (**A**, **B**), 1630 cm^{-1} (**C**, **D**), and 1618 $cm.^{-1}$ (**E**, **F**) spectral bands. Blue line: wild-type *E. coli* (W3110) in the absence of Cu ions. Red line; wild-type *E. coli* (W3110) in the presence of Cu ions. Gray line: *E. coli* porin mutants in the absence (**A**, **C**, and **E**) and presence of Cu ions (**B**, **D**, and **F**)

feature of the α-helix structures, the band at 1630 cm^{-1} is attributed to β-sheets structures. Evaluation of the band at 1652 cm^{-1} revealed no difference between the porin mutants and the wild-type bacteria in the absence of Cu ions. However, this band disappeared with Cu ions (Fig. 4A, B). The area of the 1630 cm^{-1} spectral band increased in porin mutant groups in the absence of Cu ions (Fig. 4C). This band also disappeared with the presence of Cu ions, as in the 1652 cm^{-1} band (Fig. 4D). The band 1618 cm^{-1} is also attributed to intermolecular β-sheets with solid H-bonds. Although this band did not change in porin mutant groups (Fig. 4E), its area increased in the porin mutants when exposed to Cu ions (Fig. 4F).

The IR spectra in the amide II region (1600–1400 cm^{-1}) corresponding to the proteins are shown in Fig. 5. The 1561 cm^{-1} band shows the C–C stretching from the aromatic rings. Its band area varies differently in the porin mutants compared to the wild-type bacteria in the absence of Cu ions (Fig. 5A). However, the area of this band decreased considerably

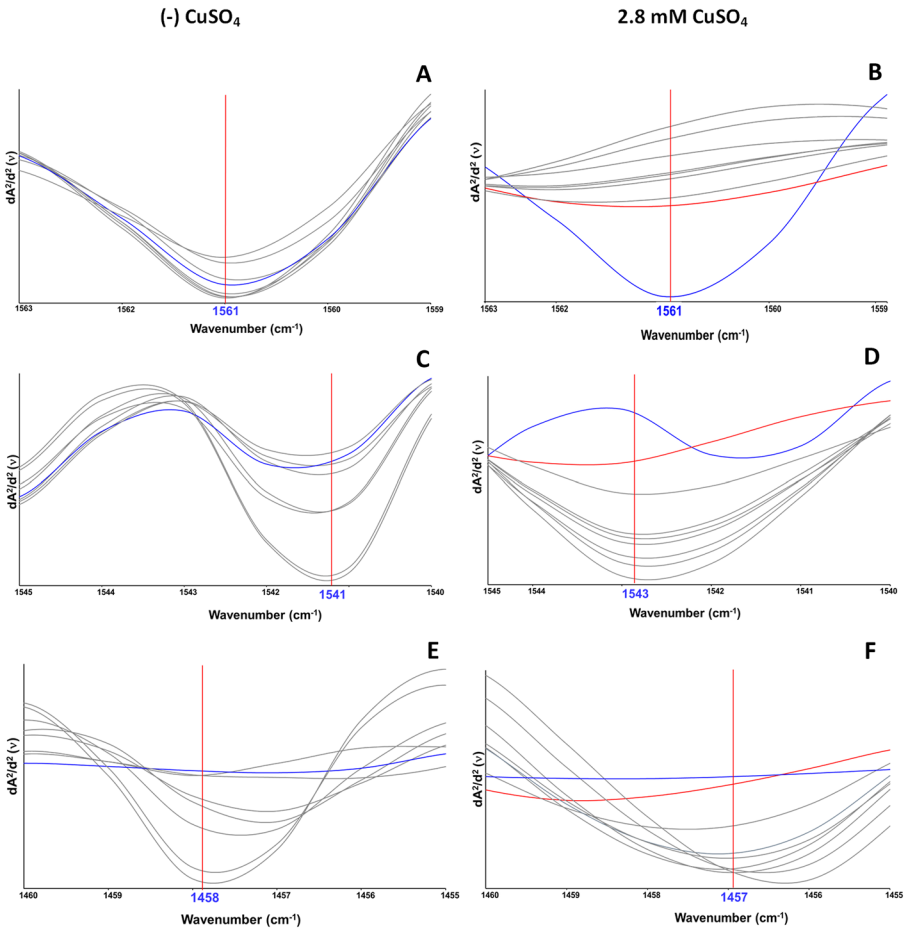

Fig. 5 Average second derivative and baseline-corrected infrared spectra of the wild-type *E. coli* (W3110) and *E. coli* porin mutants in the absence and/or presence of Cu ions for 1561 cm^{-1} (**A**, **B**), 1543–41 cm^{-1} (**C**, **D**), and 1458–57 $cm.^{-1}$ (**E**, **F**) spectral bands. Blue line: wild-type *E. coli* (W3110) in the absence of Cu ions. Red line; wild-type *E. coli* (W3110) in the presence of Cu ions. Gray line: *E. coli* porin mutants in the absence (**A**, **C**, and **E**) and presence of Cu ions (**B**, **D**, and **F**)

with the effect of Cu ions (Fig. 5B). In addition, the density of proteins corresponding to 1543–1541 cm^{-1} (N–H bending) and 1458–1457 cm^{-1} (CH_3 asymmetric) bands increased in porin mutant groups in both the absence and presence of Cu ions (Fig. 5C–F). This increase is associated with lacking porin genes unrelated to Cu ions.

3.4 Porin mutations alter bacterial DNA in the presence and absence of copper ions

The 1250–1200 cm^{-1} spectral region was analyzed to gather information about the nucleic acids, and the influential bands are presented in Fig. 6. When the wild-type *E. coli* (W3110) and its porin mutants are compared, the areas of 1245 cm^{-1} (stretching PO^{-2} symmetric vibration) and 1238 cm^{-1} (PO^{2-} antisymmetric stretching) bands are significantly increased

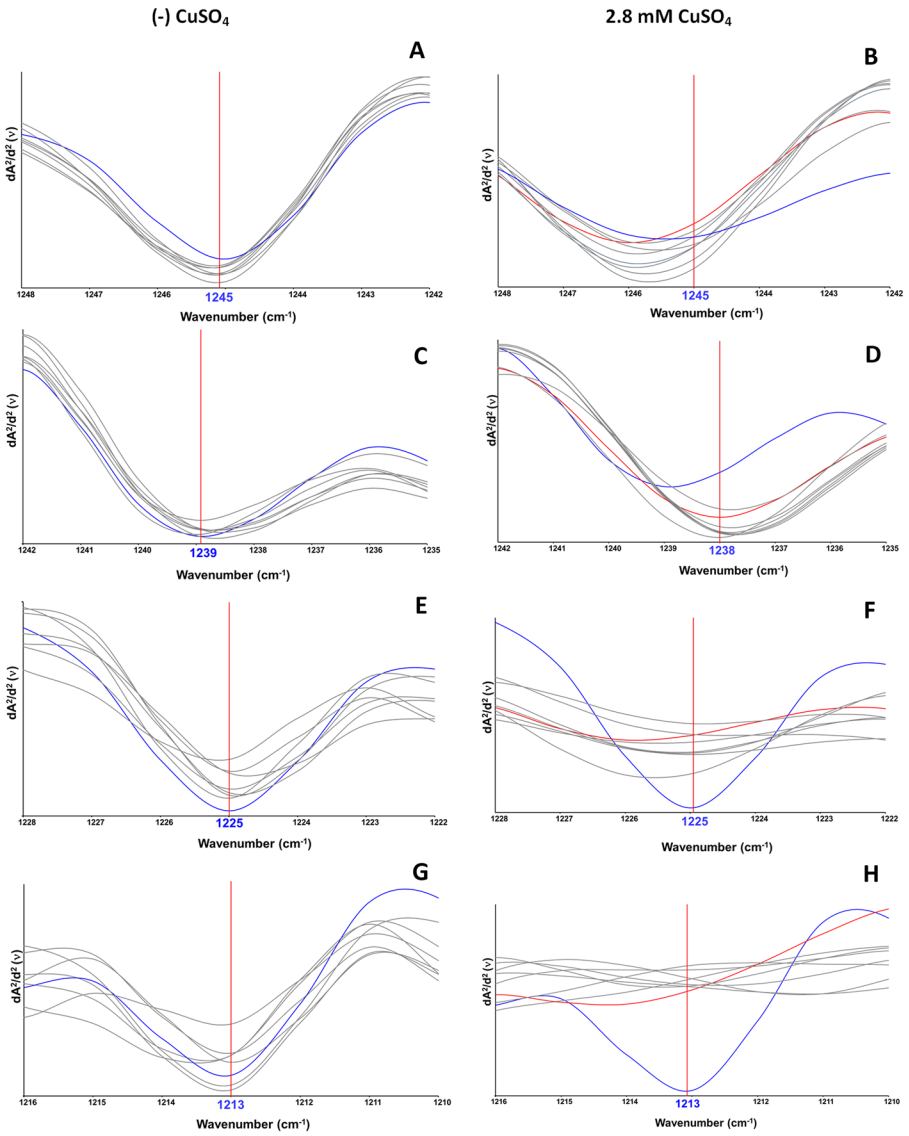

Fig. 6 Average second derivative and baseline-corrected infrared spectra of the wild-type *E. coli* (W3110) and *E. coli* porin mutants in the absence and/or presence of Cu ions for 1245 cm^{-1} (**A**, **B**), 1239–38 cm^{-1} (**C**, **D**), 1225 cm^{-1} (**E**, **F**), and 1213 $cm.^{-1}$ (**G**, **H**) spectral bands. Blue line: wild-type *E. coli* (W3110) in the absence of Cu ions. Red line; wild-type *E. coli* (W3110) in the presence of Cu ions. Gray line: *E. coli* porin mutants in the absence (**A**, **C**, and **E**) and presence of Cu ions (**B**, **D**, and **F**)

in *E. coli* porin mutants, in both the absence and presence of Cu ions (Fig. 6A–D). This increase indicates an increased concentration of A-form DNA in *E. coli* porin mutants independent of Cu ions. Moreover, positional shifts in these bands showed structural changes in DNA for bacteria exposed to Cu. The concentrations of the B-form DNA, indicated by the 1225 cm^{-1} marker band, decreased in porin mutant groups compared to wild-type bacteria

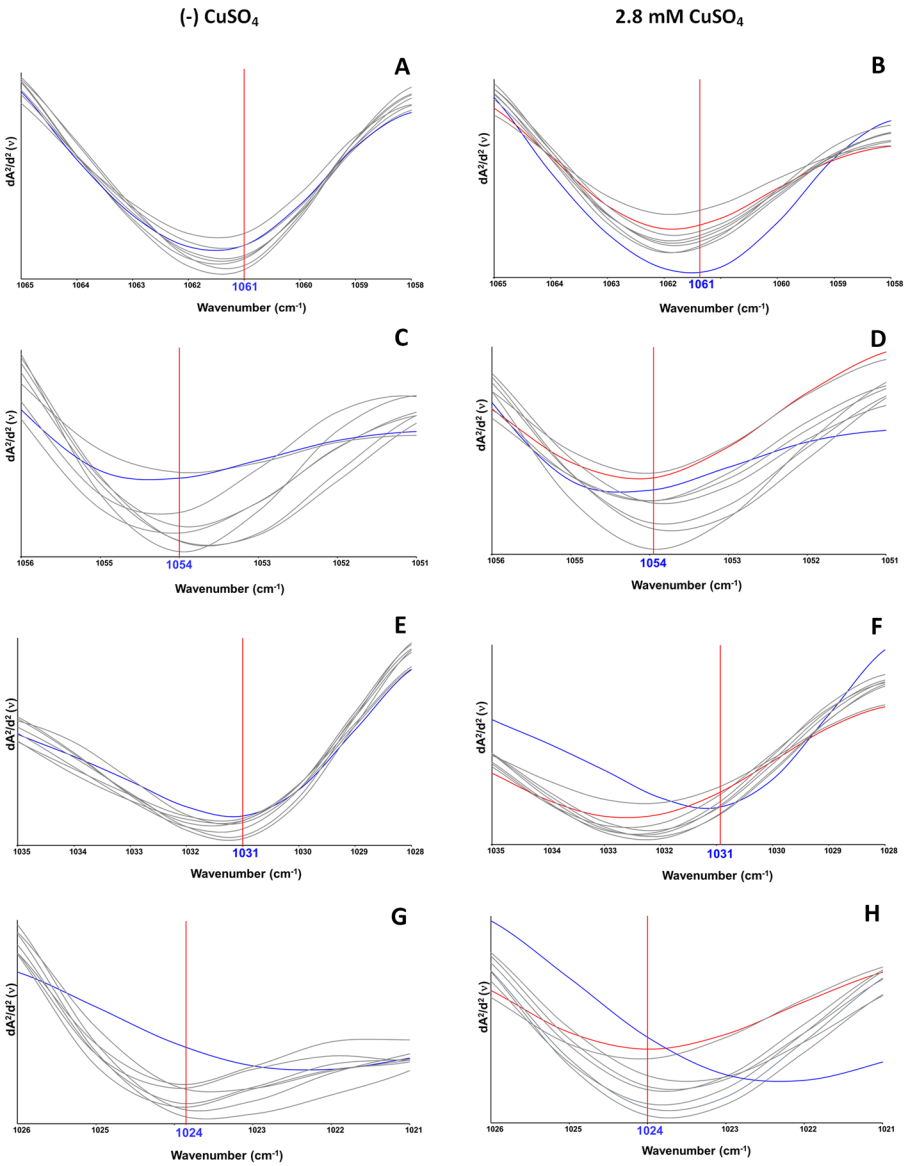

Fig. 7 Average second derivative and baseline-corrected infrared spectra of the wild-type *E. coli* (W3110) and *E. coli* porin mutants in the absence and/or presence of Cu ions for 1061 cm^{-1} (**A**, **B**), 1054 cm^{-1} (**C**, **D**), 1031 cm^{-1} (**E**, **F**), and 1024 $cm.^{-1}$ (**G**, **H**) spectral bands. Blue line: wild-type *E. coli* (W3110) in the absence of Cu ions. Red line: wild-type *E. coli* (W3110) in the presence of Cu ions. Gray line: *E. coli* porin mutants in the absence (**A**, **C**, and **E**) and presence of Cu ions (**B**, **D**, and **F**)

in the absence of Cu ions (Fig. 6E) and even disappeared with the presence of these ions (Fig. 6F). However, in the absence of Cu ions, differences in Z-form DNA represented by 1213 cm^{-1} marker band were observed between wild-type and mutant strains (Fig. 6G). A similar observation to B-DNA was depicted for Z-DNA in the presence of Cu (Fig. 6H).

Table 2 The assignment of infrared spectral bands associated with *E. coli* W3110 biomolecules

	Wavenumber (cm^{-1})	Assignment	References
1	3013–3011	C-H of lipids Unsaturated fatty acid	[55]
2	2917–2918	CH_2 antisymmetric stretching: mainly lipids Stretching C-H	[56]
3	2850	CH_2 symmetric stretching: mainly lipids	[57–59]
4	1743	Ester CO stretch: polyester storage compounds, polyhydroxyalkanoates (PHAs) Triglyceride, colesteryl esters C=O stretching mode of lipids	[60]
5	1733	Phospholipids, fatty acid ester band	[61]
6	1716	Fatty acid ester, C=O thymine	[62, 63]
7	1652	Amide I protein region (α-helix structure) -CONH- of amide I Stretching vibrations of C-O	[25, 64]
8	1630	Amide I-protein (β-sheet structure)	[65]
9	1618	Intermolecular β-sheets with strong H-bonds	[66]
10	1561	Amide protein region: C–C ring stretching; N–O stretching	[67]
11	1543–1541	Amide II absorption (primarily an N–H bending coupled to a C-N stretching vibrational mode)	[58]
12	1458–1457	Lipids and proteins (CH_3) asymmetric	[63, 68]
13	1245	A-form DNA Phosphate I (stretching PO_2^- symmetric vibration)	[56]
14	1238–1239	PO_2^- antisymmetric stretching: A-form DNA νas (PO_2^-); increased hydration of phosphate moieties (may be due to metal binding)	[69]
15	1225	PO_2^- antisymmetric stretching: B-form DNA	[56]
16	1213	Main Z-form marker PO_2^- asymmetric (phosphate I)	[56]

Table 2 (continued)

	Wavenumber (cm^{-1})	Assignment	References
17	1061	C–O stretching: polysaccharides (sulfated polysaccharides) n(CO), n(CC), d(OCH) (polysaccharides cellulose)	[70]
18	1055–1054	C-O stretching in cellulose and Hemicelluloses (C–O–C, P–O–C symmetric stretching of polysaccharides on capsule and peptidoglycan) Oligosaccharide C-O bond in hydroxyl the group that might interact with some other membrane components	[71]
19	1031	C–OH stretching vibration of primary alcohols of cellulose, poly-glucose Glycogen	[72–76]
20	1024	Stretching vibrations of C–O peaks in pyranose ring structures Glycogen (C-O stretch associated with glycogen)	[77, 78]

Table 3 Minimum inhibition concentration (*MIC*) and minimum bactericidal concentration (*MBC*) values of copper metal against wild-type *E. coli* (W3110) and *E. coli* porin mutants used in the study

Strains	MIC (µg/ml)	MBC (µg/ml)
W3110	936.38	1248.50
W3110 ompA::km	936.38	1248.50
W3110 ompC::km	624.25	936.38
W3110 ompF::km	1248.50	1872.75
W3110 ompG::km	936.38	1248.50
W3110 ompT::km	936.38	1248.50
W3110 lamB::km	1248.50	1248.50
W3110 phoE::km	936.38	1872.75

These findings demonstrate the transformations of DNA from B- and Z- to A-form due to the absence of porin genes and the presence of Cu ions.

3.5 Porin mutations alter bacterial polysaccharides in the presence and absence of copper ions

The bands located at 1061 cm^{-1} (C–O stretching: polysaccharides), 1055 cm^{-1} (C-O stretching in cellulose and hemicellulose), 1031 cm^{-1} (poly-glucose, cellulose), and 1024 cm^{-1} (C-O stretch associated with glycogen) were evaluated to understand the changes in polysaccharides under Cu exposure (Fig. 7A–H). When wild-type *E. coli* (W3110) and its porin mutants were compared, the lack of porin genes led to an increase in the polysaccharide content of bacteria in both the absence and presence of Cu ions. Bacteria increase the polysaccharide content and secrete it out of the cell to protect themselves from unfavorable environmental conditions preventing the entry of toxic products into the cell. Increased polysaccharide content helps form a biofilm-like protective layer [50]. Biofilm formation was increased without any of the porin genes, not due to the copper effect. This situation may be because the copper concentration (MIC ¾) used in the study did not show acceptable toxicity in the cell. In addition, our results also support previous studies reporting that loss of porin genes promotes biofilm formation, thus making it more tolerant to various metals [51, 52].

4 Conclusion

A very complex mechanism operates in sensing the Cu exposure in *E. coli*. Although much is known about Cu's cellular sequestration and extracellular exclusion mechanisms, the uptake events of Cu into the cell still need to be understood [53, 54]. In *E. coli*, the outer membrane is the first barrier to entering Cu into the cell. For this reason, porin proteins, which have a role in membrane permeability, are thought to have a role in transferring these ions into the cell. The changes in lipids, proteins, fatty acids, nucleic acids, and polysaccharides of wild-type *E. coli* and its porin-deficient mutant strains were identified in the presence and absence of Cu ions by infrared spectroscopic analyses. Accordingly, both structural variations in lipid components and an increase in the concentration of lipid molecules were observed in all porin mutants. There was a diminished number of lipid molecules in wild-type *E. coli* (W3110) exposed to Cu, while the absence of porin genes increased

lipid concentrations. The lack of porin genes significantly elevated the amounts of fatty acids and phospholipids in the absence and presence of Cu ions. This situation indicates that membrane integrity is impaired in porin mutant cells. When the alterations in protein secondary structures were compared, the quantity of amide I proteins directly related to the protein backbone conformation was diminished by the presence of Cu ions. On the other hand, the amount of amide II proteins increased in porin mutant groups independent of Cu ion presence or absence. Moreover, the lack of porin genes seriously affected the conformational structures of the proteins. In the case of nucleic acids, the DNAs are transformed from B- and Z-form to A-form due to porin mutations and the presence of Cu ions. The absence of porin genes increased polysaccharide content independent of Cu presence. The study is valuable for investigating the link between Cu exposure and biomolecular changes in porin mutant and wild-type bacterial cells to understand the role of bacterial porin proteins in Cu exposure for the first time.

Bacteria cannot change the number of porin proteins in the membrane under various stress conditions. Still, they can show the ability to narrow and open the pore size to balance the physiological homeostasis of the cell. Thus, cells protect themselves against harmful molecules by increasing or decreasing the pore diameter. This study will provide insight into future studies in which porin genes are associated with copper ion uptake or excretion. Therefore, study findings can also help characterize Cu detoxification efficiency and guide obtaining active living cells for bioremediation. Bioremediation is an emerging technology that removes, attenuates, or converts pollutants using living organisms. Similarly known as biodegradation, this technology uses biological processes and can be efficiently monitored by FTIR spectroscopy. FTIR spectroscopy is essential for these kinds of studies because it is low-cost, not time-consuming, and applicable to various materials. It also provides molecular-level data on a sample's organic components and is a proven method for simultaneously investigating microbial metabolic processes.

Acknowledgements The authors thank the Department of Molecular Biology and Genetics (for providing the laboratory facilities) and the Department of Chemistry (for providing an FTIR spectrometer) at Bilecik Şeyh Edebali University.

Author contribution All the authors contributed to the conception and design of the study. This study is part of the Ph.D. thesis of Gulcin Cetin Kilicaslan under the supervision of Cihan Darcan. Gulcin Cetin Kilicaslan conducted the experiments with help from Rafig Gurbanov. Gulcin Cetin Kilicaslan and Rafig Gurbanov analyzed the results and wrote the manuscript. The final manuscript has been read and approved by all the authors.

Funding This work is supported by the Scientific Research Project Fund of BİLECİK ŞEYH EDEBALİ ÜNİVERSİTESİ under the project number 2015–01.BŞEÜ.04–02 to CD.

Data Availability The datasets generated during and/or analysed during the current study are available from the corresponding author on reasonable request.

Declarations

Ethical approval This is a bacteriological study. No ethical approval is required.

Informed consent Not applicable.

Conflict of interest The authors declare no competing interests.

References

1. Porcheron, G., Garénaux, A., Proulx, J., Sabri, M., Dozois, C.M.: Iron, copper, zinc, and manganese transport and regulation in pathogenic Enterobacteria: Correlations between strains, site of infection and the relative importance of the different metal transport systems for virulence. Front. Cell. Infect. Microbiol. **3** (2013). https://doi.org/10.3389/fcimb.2013.00090
2. Waldron, K.J., Robinson, N.J.: How do bacterial cells ensure that metalloproteins get the correct metal?. Nat. Rev. Microbiol. **7**, 25–35 (2009). https://doi.org/10.1038/nrmicro2057
3. Chandrangsu, P., Rensing, C., Helmann, J.D.: Erratum: Metal homeostasis and resistance in bacteria. Nat. Rev. Microbiol. **15** (2017). https://doi.org/10.1038/nrmicro.2017.53
4. Bruins, M.R., Kapil, S., Oehme, F.W.: Microbial resistance to metals in the environment. Ecotoxicol. Environ. Saf. **45**, 198–207 (2000). https://doi.org/10.1006/eesa.1999.1860
5. Baksh, K.A., Zamble, D.B.: Allosteric control of metal-responsive transcriptional regulators in bacteria. J Biol Chem. **295**, 1673–1684 (2020). https://doi.org/10.1074/jbc.REV119.011444
6. Hohl, H., Varma, A.: Soil-The Living Matrix. In: Soil Heavy Metals. I. Sherameti, I., Varma, A. (eds.) Soil Biology, pp. 1–18. Springer-Verlag, Berlin, Heidelberg (2010)
7. Dixit, R., Wasiullah, Malaviya, D., Pandiyan, K., Singh, U.B., Sahu, A., Shukla, R., Singh, B.P., Rai, J.P., Sharma, P.K., Lade, H., Paul, D.: Bioremediation of heavy metals from soil and aquatic environment: An overview of principles and criteria of fundamental processes, Sustainability **7**, 2189–2212 (2015). https://doi.org/10.3390/su7022189
8. Capdevila, D.A., Edmonds, K.A., Giedroc, D.P.: Metallochaperones and metalloregulation in bacteria. Essays. Biochem. **61**, 177–200 (2017). https://doi.org/10.1042/EBC20160076
9. Henderson, J.C., Zimmerman, S.M., Crofts, A.A., Boll, J.M., Kuhns, L.G., Herrera, C.M., Trent, M.S.: The power of asymmetry: architecture and assembly of the gram-negative outer membrane lipid bilayer. Annu. Rev. Microbiol. **70**, 255–278 (2016). https://doi.org/10.1146/annurev-micro-102215-095308
10. O'Shea, R., Moser, H.E.: Physicochemical properties of antibacterial compounds: Implications for drug discovery. J. Med. Chem. **51** (2008). https://doi.org/10.1021/jm700967e
11. Chudobova, D., Dostalova, S., Ruttkay-Nedecky, B., Guran, R., Rodrigo, M.A.M., Tmejova, K., Krizkova, S., Zitka, O., Adam, V., Kizek, R.: The effect of metal ions on Staphylococcus aureus revealed by biochemical and mass spectrometric analyses. Microbiol. Res. 170 (2015). https://doi.org/10.1016/j.micres.2014.08.003
12. Nanda, M., Kumar, V., Sharma, D.K.: Multimetal tolerance mechanisms in bacteria: The resistance strategies acquired by bacteria that can be exploited to 'clean-up' heavy metal contaminants from water. Aquat. Toxicol. **212**, 1–10 (2019). https://doi.org/10.1016/j.aquatox.2019.04.011
13. Gurbanov, R., Gozen, A.G., Severcan, F.: Rapid classification of heavy metal-exposed freshwater bacteria by infrared spectroscopy coupled with chemometrics using supervised method. Spectrochim. Acta. Mol. Biomol. Spectrosc. **189**, 282–290 (2018). https://doi.org/10.1016/j.saa.2017.08.038
14. Gurbanov, R., Tunçer, S., Mingu, S., Severcan, F., Gozen, A.G.: Methylation, sugar puckering and Z-form status of DNA from a heavy metal-acclimated freshwater *Gordonia* sp. J. Photochem. Photobiol. B **198** (2019). https://doi.org/10.1016/j.jphotobiol.2019.111580
15. Gurbanov, R., Karadağ, H., Karaçam, S., Samgane, G.: Tapioca starch modulates cellular events in oral probiotic *Streptococcus salivarius* strains. Probiotics Antimicrob. Proteins (2021). https://doi.org/10.1007/s12602-020-09678-z
16. Sykora, L., Müller, A.: ATR-FTIR Microplate Reader and Micromachined ATR Silicon Crystals. 11th Workshop FT-IR Spectroscopy in Microbiological and Medical Diagnostics **199** (2017)
17. Sharma, P., Pandey, A.K., Kim, S.H., Singh, S.P., Chaturvedi, P., Varjani, S.: Critical review on microbial community during in-situ bioremediation of heavy metals from industrial wastewater. Environ. Technol. Innov. **24** (2021). https://doi.org/10.1016/j.eti.2021.101826
18. Wenning, M., Scherer, S.: Identification of microorganisms by FTIR spectroscopy: Perspectives and limitations of the method. Appl. Microbiol. Biotechnol. **97**, 7111–7120 (2013). https://doi.org/10.1007/s00253-013-5087-3
19. Alvarez-Ordóñez, A., Mouwen, D.J.M., López, M., Prieto, M.: Fourier transform infrared spectroscopy as a tool to characterize molecular composition and stress response in foodborne pathogenic bacteria. J. Microbiol. Methods **84**, 369–378 (2011). https://doi.org/10.1016/j.mimet.2011.01.009
20. Al-Qadiri, H.M., Al-Alami, N.I., Al-Holy, M.A., Rasco, B.A.: Using Fourier transform infrared (FT-IR) absorbance spectroscopy and multivariate analysis to study the effect of chlorine-induced bacterial injury in water. J. Agric. Food Chem. **56**, (2008). https://doi.org/10.1021/jf801604p
21. Davis, R., Mauer, L.: Fourier transform infrared (FT-IR) spectroscopy: a rapid tool for detection and analysis of foodborne pathogenic bacteria. Current Research, Technology and Education Topics in Applied Microbiology and Microbial Biotechnology. A. Méndez-Vilas (ed.). (2010)

22. Basnet, P., Amarasiriwardena, D., Wu, F., Fu, Z., Zhang, T.: Investigation of tissue level distribution of functional groups and associated trace metals in rice seeds (*Oryza sativa* L.) using FTIR and LA-ICP-MS. Microchem. J. **127** (2016). https://doi.org/10.1016/j.microc.2016.02.020
23. Jiao, Y., Cody, G.D., Harding, A.K., Wilmes, P., Schrenk, M., Wheeler, K.E., Banfield, J.F., Thelen, M.P.: Characterization of extracellular polymeric substances from acidophilic microbial biofilms. Appl. Environ. Microbiol. **76** (2010). https://doi.org/10.1128/AEM.02289-09
24. Gurbanov, R., Simsek Ozek, N., Gozen, A.G., Severcan, F.: Quick discrimination of heavy metal resistant bacterial populations using infrared spectroscopy coupled with chemometrics. Anal. Chem. **87**, 9653–9661 (2015). https://doi.org/10.1021/acs.analchem.5b01659
25. Pradhan, S., Singh, S., Rai, L.C.: Characterization of various functional groups present in the capsule of Microcystis and study of their role in biosorption of Fe, Ni and Cr. Bioresour. Technol. **98**, 595–601 (2007). https://doi.org/10.1016/j.biortech.2006.02.041
26. Saranya, K., Sundaramanickam, A., Shekhar, S., Meena, M., Sathishkumar, R.S., Balasubramanian, T.: Biosorption of multi-heavy metals by coral associated phosphate solubilising bacteria *Cronobacter muytjensii* KSCAS2. J. Environ. Manage. **222**, 396–401 (2018). https://doi.org/10.1016/j.jenvman.2018.05.083
27. Rengel, Z., Marschner, P.: Nutrient availability and management in the rhizosphere: Exploiting genotypic differences. New Phytol. **168**, 305–312 (2005). https://doi.org/10.1111/j.1469-8137.2005.01558.x
28. Koebnik, R., Locher, K.P., van Gelder, P.: Structure and function of bacterial outer membrane proteins: barrels in a nutshell. Mol. Microbiol. **37**, 239–253 (2000). https://doi.org/10.1046/j.1365-2958.2000.01983.x
29. Nikaido, H.: Molecular basis of bacterial outer membrane permeability revisited. Microbiol. Mol. Biol. Rev. **67**, 593–656 (2003). https://doi.org/10.1128/MMBR.67.4.593-656.2003
30. Samsudin, F., Boags, A., Piggot, T.J., Khalid, S.: Braun's lipoprotein facilitates OmpA interaction with the *Escherichia coli* cell wall. Biophys. J. **113**, 1496–1504 (2017). https://doi.org/10.1016/j.bpj.2017.08.011
31. Park, J.S., Lee, W.C., Yeo, K.J., Ryu, K., Kumarasiri, M., Hesek, D., Lee, M., Mobashery, S., Song, J.H., Kim, S. il, Lee, J.C., Cheong, C., Jeon, Y.H., Kim, H.: Mechanism of anchoring of OmpA protein to the cell wall peptidoglycan of the gram-negative bacterial outer membrane. FASEB J. **26**, 219–228 (2012). https://doi.org/10.1096/fj.11-188425
32. Smith, S.G.J., Mahon, V., Lambert, M.A., Fagan, R.P.: A molecular Swiss army knife: OmpA structure, function and expression. FEMS Microbiol. Lett. **273**, 1–11 (2007). https://doi.org/10.1111/j.1574-6968.2007.00778.x
33. Ebbensgaard, A., Mordhorst, H., Aarestrup, F.M., Hansen, E.B.: The role of outer membrane proteins and lipopolysaccharides for the sensitivity of *Escherichia coli* to antimicrobial peptides. Front. Microbiol. **9** (2018). https://doi.org/10.3389/fmicb.2018.02153
34. Wang, J., Ma, W., Wang, X.: Insights into the structure of *Escherichia coli* outer membrane as the target for engineering microbial cell factories. Microb. Cell. Fact. **20**, 73 (2021). https://doi.org/10.1186/s12934-021-01565-8
35. Wimley, W.C.: The versatile β-barrel membrane protein. Curr. Opin. Struct. Biol. **13**, 404–411 (2003). https://doi.org/10.1016/S0959-440X(03)00099-X
36. Vergalli, J., Bodrenko, I. v., Masi, M., Moynié, L., Acosta-Gutiérrez, S., Naismith, J.H., Davin-Regli, A., Ceccarelli, M., van den Berg, B., Winterhalter, M., Pagès, J.-M.: Porins and small-molecule translocation across the outer membrane of Gram-negative bacteria. Nat. Rev. Microbiol. **18**, 164–176 (2020). https://doi.org/10.1038/s41579-019-0294-2
37. Fernández, L., Hancock, R.E.W.: Adaptive and mutational resistance: role of porins and efflux pumps in drug resistance. Clin. Microbiol. Rev. **25**, 661–681 (2012). https://doi.org/10.1128/CMR.00043-12
38. Pagès, J.-M., James, C.E., Winterhalter, M.: The porin and the permeating antibiotic: a selective diffusion barrier in Gram-negative bacteria. Nat. Rev. Microbiol. **6**, 893–903 (2008). https://doi.org/10.1038/nrmicro1994
39. Low, A.S., MacKenzie, F.M., Gould, I.M., Booth, I.R.: Protected environments allow parallel evolution of a bacterial pathogen in a patient subjected to long-term antibiotic therapy. Mol. Microbiol. **42**, 619–630 (2008). https://doi.org/10.1046/j.1365-2958.2001.02647.x
40. Ruffing, A.M.: RNA-Seq analysis and targeted mutagenesis for improved free fatty acid production in an engineered cyanobacterium. Biotechnol. Biofuels. **6**, 113 (2013). https://doi.org/10.1186/1754-6834-6-113
41. Arunmanee, W., Pathania, M., Solovyova, A.S., le Brun, A.P., Ridley, H., Baslé, A., van den Berg, B., Lakey, J.H.: Gram-negative trimeric porins have specific LPS binding sites that are essential for porin biogenesis. Proc Natl. Acad Sci. U.S.A. **113**, (2016). https://doi.org/10.1073/pnas.1602382113
42. Ma, Y., Rajkumar, M., Freitas, H.: Improvement of plant growth and nickel uptake by nickel resistant-plant-growth promoting bacteria. J. Hazard. Mater. **166**, (2009). https://doi.org/10.1016/j.jhazmat.2008.12.018

43. Yam, C.H., Siu, W.Y., Kaganovich, D., Ruderman, J.V., Poon, R.Y.C.: Cleavage of cyclin A at R70/R71 by the bacterial protease OmpT. Proc Natl. Acad Sci. U.S.A. **98**, 497–501 (2001). https://doi.org/10.1073/pnas.98.2.497
44. Xu, Y., Tan, L., Li, Q., Zheng, X., Liu, W.: Sublethal concentrations of heavy metals Cu^{2+} and Zn^{2+} can induce the emergence of bacterial multidrug resistance. Environ. Technol. Innov. **27**, 102379 (2022). https://doi.org/10.1016/j.eti.2022.102379
45. Sato, M., Machida, K., Arikado, E., Saito, H., Kakegawa, T., Kobayashi, H.: Expression of Outer Membrane Proteins in *Escherichia coli* Growing at Acid pH. Appl. Environ. Microbiol. **66**, 943–947 (2000). https://doi.org/10.1128/AEM.66.3.943-947.2000
46. Miller, J.F., Johnson, S.A., Black, W.J., Beattie, D.T., Mekalanos, J.J., Falkow, S.: Constitutive sensory transduction mutations in the *Bordetella pertussis* bvgS gene. J. Bacteriol. **174** (1992). https://doi.org/10.1128/jb.174.3.970-979.1992
47. Jiang, C., Sheng, X., Qian, M., Wang, Q.: Isolation and characterization of a heavy metal-resistant Burkholderia sp. from heavy metal-contaminated paddy field soil and its potential in promoting plant growth and heavy metal accumulation in metal-polluted soil. Chemosphere **72**, 157–164 (2008). https://doi.org/10.1016/j.chemosphere.2008.02.006
48. Gupta, A.D., Kavitha, E., Singh, S., Karthikeyan, S.: Toxicity mechanism of Cu^{2+} ion individually and in combination with Zn^{2+} ion in characterizing the molecular changes of *Staphylococcus aureus* studied using FTIR coupled with chemometric analysis. J. Biol. Phys. **46**, (2020). https://doi.org/10.1007/s10867-020-09560-7
49. Goswami, L., Arul Manikandan, N., Pakshirajan, K., Pugazhenthi, G.: Simultaneous heavy metal removal and anthracene biodegradation by the oleaginous bacteria *Rhodococcus opacus*. 3 Biotech. **7**, 37 (2017). https://doi.org/10.1007/s13205-016-0597-1
50. Limoli, D.H., Jones, C.J., Wozniak, D.J.: Bacterial extracellular polysaccharides in biofilm formation and function. Microbiol. Spectr. **3** (2015). https://doi.org/10.1128/microbiolspec.mb-0011-2014
51. Radzig, M.A., Koksharova, O.A., Khmel', I.A.: Antibacterial effects of silver ions on growth of gram-negative bacteria and biofilm formation. Mol. Genet. Microbiol. Virol. **24**, 194–199 (2009). https://doi.org/10.3103/S0891416809040065
52. Markova, J.A., Anganova, E.V., Turskaya, A.L., Bybin, V.A., Savilov, E.D.: Regulation of *Escherichia coli* biofilm formation. Appl. Biochem Microbiol. **54** (2018). https://doi.org/10.1134/S0003683818010040
53. Solioz, M.: Copper and Bacteria Evolution, Homeostasis and Toxicity. Springer (2018)
54. Argüello, J.M., Raimunda, D., Padilla-Benavides, T.: Mechanisms of copper homeostasis in bacteria. Front. Cell. Infect. Microbiol. **4** (2013). https://doi.org/10.3389/fcimb.2013.00073
55. Fung, M.F.K., Senterman, M.K., Mikhael, N.Z., Lacelle, S., Wong, P.T.T.: Pressure-tuning Fourier transform infrared spectroscopic study of carcinogenesis in human endometrium. Biospectroscopy (1996). https://doi.org/10.1002/(SICI)1520-6343(1996)2:3<155::AID-BSPY2>3.0.CO;2-7
56. Movasaghi, Z., Rehman, S., ur Rehman, D.I.: Fourier Transform Infrared (FTIR) Spectroscopy of biological tissues. Appl. Spectrosc. Rev. **43**, 134–179 (2008). https://doi.org/10.1080/05704920701829043
57. Cakmak, G., Togan, I., Severcan, F.: 17β-Estradiol induced compositional, structural and functional changes in rainbow trout liver, revealed by FT-IR spectroscopy: A comparative study with nonylphenol. Aquat. Toxicol. **77**, 53–63 (2006). https://doi.org/10.1016/j.aquatox.2005.10.015
58. Simsek Ozek, N., Bal, I.B., Sara, Y., Onur, R., Severcan, F.: Structural and functional characterization of simvastatin-induced myotoxicity in different skeletal muscles. Biochim Biophys Acta Gen. Subj. **1840** (2014). https://doi.org/10.1016/j.bbagen.2013.09.010
59. Naumann, D.: FT-Infrared and FT-Raman spectroscopy in biomedical research. Appl. Spectrosc. Rev. **36**, 239–298 (2001). https://doi.org/10.1081/ASR-100106157
60. Vongsvivut, J., Miller, M.R., McNaughton, D., Heraud, P., Barrow, C.J.: Rapid discrimination and determination of polyunsaturated fatty acid composition in marine oils by FTIR spectroscopy and multivariate data analysis. Food Bioproc. Tech. **7**, (2014). https://doi.org/10.1007/s11947-013-1251-0
61. Yoshida, S., Miyazaki, M., Sakai, K., Takeshita, M., Yuasa, S., Sato, A., Kobayashi, T., Watanabe, S., Okuyama, H.: Fourier transform infrared spectroscopic analysis of rat brain microsomal membranes modified by dietary fatty acids: Possible correlation with altered learning behavior. Biospectroscopy **3**, 281–290 (1997). https://doi.org/10.1002/(SICI)1520-6343(1997)3:4<281::AID-BSPY3>3.0.CO;2-7
62. Dovbeshko, G.I., Gridina, N.Y., Kruglova, E.B., Pashchuk, O.P.: FTIR spectroscopy studies of nucleic acid damage. Talanta. **53**, 233–246 (2000). https://doi.org/10.1016/S0039-9140(00)00462-8
63. Fabian, H., Jackson, M., Murphy, L., Watson, P.H., Fichtner, I., Mantsch, H.H.: A comparative infrared spectroscopic study of human breast tumors and breast tumor cell xenografts. Biospectroscopy (1995). https://doi.org/10.1002/bspy.350010106

64. Abbott, G.W., Ramesh, B., Srai, S.K.: Interaction between soluble and membrane-embedded potassium channel peptides monitored by Fourier transform infrared spectroscopy. PLoS One (2012). https://doi.org/10.1371/journal.pone.0049070
65. Varotsis, C., Papageorgiou, M., Tselios, C., Yiannakkos, K.A., Adamou, A., Nicolaides, A.: Bacterial colonization on the surface of copper sulfide minerals probed by fourier transform infrared micro-spectroscopy. Crystals (Basel). **10**, 1–10 (2020). https://doi.org/10.3390/cryst10111002
66. Piccirilli, F., Schirò, G., Vetri, V., Lupi, S., Perucchi, A., Militello, V.: Decoding vibrational states of Concanavalin A amyloid fibrils. Biophys. Chem. **199**, (2015). https://doi.org/10.1016/j.bpc.2015.02.007
67. Wei, S., Liu, J., Xia, Y., Zhang, H., Cheng, R., Sun, L., Xu, F., Huang, P., Rosei, F., Pimerzin, A.A., Seifert, H.J., Pan, H.: Remarkable catalysis of spinel ferrite XFe_2O_4 (X = Ni, Co, Mn, Cu, Zn) nanoparticles on the dehydrogenation properties of $LiAlH_4$: An experimental and theoretical study. J. Mater. Sci. Technol. **111**, (2022). https://doi.org/10.1016/j.jmst.2021.08.088
68. Fujioka, N., Morimoto, Y., Arai, T., Kikuchi, M.: Discrimination between normal and malignant human gastric tissues by Fourier transform infrared spectroscopy. Cancer. Detect. Prev. **28** (2004). https://doi.org/10.1016/j.cdp.2003.11.004
69. Fukuyama, Y., Yoshida, S., Yanagisawa, S., Shimizu, M.: A study on the differences between oral squamous cell carcinomas and normal oral mucosas measured by Fourier transform infrared spectroscopy. Biospectroscopy. **5**, 117–126 (1999). https://doi.org/10.1002/(SICI)1520-6343(1999)5:2<117::AID-BSPY5>3.0.CO;2-K
70. Caputo, H.E., Straub, J.E., Grinstaff, M.W.: Design, synthesis, and biomedical applications of synthetic sulphated polysaccharides. Chem. Soc. Rev. **8** (2019). https://doi.org/10.1039/C7CS00593H
71. Quilès, F., Humbert, F., Delille, A.: Analysis of changes in attenuated total reflection FTIR fingerprints of Pseudomonas fluorescens from planktonic state to nascent biofilm state. Spectrochim. Acta. Mol. Biomol. Spectrosc. **75** (2010). https://doi.org/10.1016/j.saa.2009.11.026
72. Delille, A., Quilès, F., Humbert, F.: In situ monitoring of the nascent *Pseudomonas fluorescens* biofilm response to variations in the dissolved organic carbon level in low-nutrient water by attenuated total reflectance-Fourier transform infrared spectroscopy. Appl. Environ. Microbiol. **73** (2007). https://doi.org/10.1128/AEM.00838-07
73. Workman, J.J.: Infrared and Raman spectroscopy in paper and pulp analysis. Appl. Spectrosc. Rev. **36**, 139–168 (2001). https://doi.org/10.1081/ASR-100106154
74. Ngo Thi, N.A., Naumann, D.: Investigating the heterogeneity of cell growth in microbial colonies by FTIR microspectroscopy. Anal. Bioanal. Chem. **387**, 1769–1777 (2007). https://doi.org/10.1007/s00216-006-0829-z
75. Ostrowska, K.M., Garcia, A., Meade, A.D., Malkin, A., Okewumi, I., O'Leary, J.J., Martin, C., Byrne, H.J., Lyng, F.M.: Correlation of p16INK4A expression and HPV copy number with cellular FTIR spectroscopic signatures of cervical cancer cells. Analyst. **136** (2011). https://doi.org/10.1039/c0an00910e
76. Holman, H.Y.N., Bechtel, H.A., Hao, Z., Martin, M.C.: Synchrotron IR spectromicroscopy: Chemistry of living cells. Anal. Chem. **82** (2010). https://doi.org/10.1021/ac100991d
77. Wood, B.R., Quinn, M.A., Burden, F.R., McNaughton, D.: An investigation into FTIR spectroscopy as a biodiagnostic tool for cervical cancer. Biospectroscopy **2**, 497–498 (1996). https://doi.org/10.1002/(SICI)1520-6343(1996)2:3<143::AID-BSPY1>3.0.CO;2-9
78. Wood, B.R., Quinn, M.A., Tait, B., Ashdown, M., Hislop, T., Romeo, M., McNaughton, D.: FTIR microspectroscopic study of cell types and potential confounding variables in screening for cervical malignancies. Biospectroscopy **4**, 75–91 (1998). https://doi.org/10.1002/(SICI)1520-6343(1998)4:2<75::AID-BSPY1>3.0.CO;2-R